5390 *Biochemistry* **2010,** *49,* 5390–5396
DOI: 10.1021/bi100761x

BIOCHEMISTRY
including biophysical chemistry & molecular biology
Article

The Temperature Dependence of the Kinetic Isotope Effects of Dihydrofolate Reductase from *Thermotoga maritima* Is Influenced by Intersubunit Interactions[†]

E. Joel Loveridge and Rudolf K. Allemann*

School of Chemistry, Cardiff University, Main Building, Park Place, Cardiff CF10 3AT, United Kingdom

Received May 13, 2010; Revised Manuscript Received May 29, 2010

ABSTRACT: Dihydrofolate reductase from the hyperthermophile *Thermotoga maritima* (TmDHFR) is unique among structurally characterized chromosomal DHFRs in that it forms a stable homodimer. Dimerization is believed to play a key role in the high thermal stability of TmDHFR, which is reflected in a melting temperature in excess of 85 °C. The dimer interface of TmDHFR is composed of a hydrophobic core with charged residues around the periphery. In particular, Lys129 of each subunit forms three-membered salt bridges with Glu136 and Glu138 of the other subunit. To probe the role of these salt bridges in the dimerization and thermal stability of TmDHFR, we generated a series of variants (TmDHFR-K129E, TmDHFR-E136K, TmDHFR-E138K, and TmDHFR-E136K/E138K) in which these residues were exchanged for residues whose side chains bear the opposite charge. Our results indicate that these salt bridges are key for the high thermal stability of TmDHFR but are not a requirement for dimerization. Although the rate of dihydrofolate reduction by TmDHFR is not significantly affected by the loss of the K129−E136−E138 salt bridges, changes to the temperature dependence of the kinetic isotope effect on hydride transfer are observed. These changes are in agreement with the proposal that DHFR catalysis may be affected by changes to the conformational ensemble of the enzyme rather than only to the coupling of protein motions to the reaction coordinate.

Dihydrofolate reductase (DHFR)[1] catalyzes the reduction of 7,8-dihydrofolate (H_2F) to 5,6,7,8-tetrahydrofolate using reduced nicotinamide adenine dinucleotide phosphate (NADPH) as a cofactor. Its central position in metabolism and subsequent pharmacological importance has led to the characterization of DHFRs from more than 30 species and all three kingdoms of life. DHFR has become central to the study of the relationship between enzyme structure, dynamics, and catalysis (*1*−*7*).

DHFR from the hyperthermophilic bacterium *Thermotoga maritima* (TmDHFR), in contrast to all other structurally characterized chromosomal DHFRs, forms a stable homodimer (*8*), although it maintains a tertiary structure similar to that of monomeric DHFRs (*9*). TmDHFR is the most thermostable DHFR that has been isolated (*8*, *10*, *11*), with a melting temperature approximately 30 °C above that of the *Escherichia coli* enzyme (*12*). We have recently shown that the dimeric structure of TmDHFR is critical to its high thermostability (*13*). In addition, TmDHFR binds its ligands more tightly than other DHFRs, which is likely to reflect an adaptation to life at extreme temperatures (*14*). TmDHFR has a low catalytic turnover rate compared to its mesophilic homologues, which had been postulated to be due to dimerization (*12*). However, a monomeric version of TmDHFR, in which Val11 had been replaced by aspartate, was characterized by a reduced steady-state turnover rate but did not show a change in the rate of hydride transfer (*13*) in contrast to previous proposals (*12*, *15*). Similarly, engineered monomeric variants of phosphoribosylanthranilate isomerase from *T. maritima* have been shown to have reduced thermostability but identical catalytic activities compared to those of the dimeric wild-type enzyme (*16*).

Both ion pair formation and oligomerization have been shown to play a role in increasing protein thermostability (*17*), although structural genomics analysis revealed no overall increase in the level of protein oligomerization in *T. maritima* relative to mesophilic species (*18*). Intramolecular ion pairs have been shown to be important for thermostability in both indoleglycerol phosphate synthase (*19*) and glyceraldehyde-3-phosphate dehydrogenase (*20*) from *T. maritima*. An intersubunit salt bridge is important for tetramerization and high thermostability in a quinone reductase from *Bacillus subtilis* (*21*), while an intersubunit ion pair contributes to the thermostability of glutamate dehydrogenase (*22*, *23*). A recent study of mesophilic−thermophilic alcohol dehydrogenase chimeras found that the thermal stability could be improved significantly through the incorporation of intersubunit ion pairs (*24*).

The dimer interface of TmDHFR is predominantly composed of hydrophobic residues, with charged residues around the periphery (Figure 1) (*9*). Lys129 of one subunit forms a three-membered salt bridge with Glu136 and Glu138 of the other subunit, which was proposed to play a significant role in

[†]This work was supported by the Biotechnology and Biological Sciences Research Council (BBSRC) through Grant BB/E008380/1, the University of Birmingham, and Cardiff University.

*To whom correspondence should be addressed: School of Chemistry, Cardiff University, Main Building, Park Place, Cardiff CF10 3AT, United Kingdom. Phone: (44) 29 2087 9014. Fax: (44) 29 2087 4030. E-mail: allemannrk@cf.ac.uk.

[1]Abbreviations: DHFR, dihydrofolate reductase; EcDHFR, DHFR from *Escherichia coli*; TmDHFR, DHFR from *Thermotoga maritima*; NADPH, nicotinamide adenine dinucleotide phosphate; TbADH, alcohol dehydrogenase from *Thermoanaerobacter brockii*; H_2F, 7,8-dihydrofolate; CHAPS, 3-[(3-cholamidopropyl)dimethylammonio]-1-propanesulfonate; KIE, kinetic isotope effect; CD, circular dichroism; SEC, size exclusion chromatography.

 Published on Web 06/01/2010

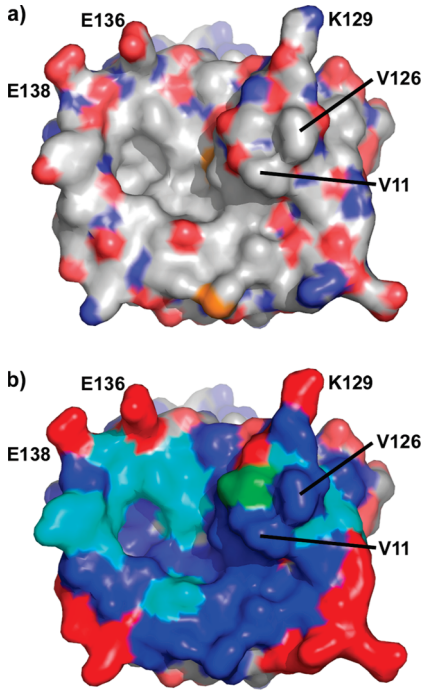

FIGURE 1: Surface representation of the TmDHFR dimer interface created from Protein Data Bank entry 1D1G (*9*) using PyMOL. In panel a, the colors represent carbon (gray), nitrogen (blue), oxygen (red), and sulfur (orange); in panel b, they represent aliphatic apolar (blue), aromatic (cyan), polar uncharged (green), and charged (red) residues.

thermostability (*9*). Computational results suggest that this region of TmDHFR retains the native structure until late in the unfolding process (*25*), also implying that this salt bridge is important for thermostability. We have previously reported that single or double mutation of Glu136 and Glu138 to lysine residues does not affect dimerization of TmDHFR (*1*). Here we demonstrate that while these Lys129−Glu136−Glu138 salt bridges do not play a significant role in dimer formation, they are nevertheless vital for the high thermostability of TmDHFR, and we consider their effect on the catalytic function of TmDHFR.

MATERIALS AND METHODS

Chemicals. NADPH and $NADP^+$ were purchased from Melford. Folate, d^8-2-propanol, and alcohol dehydrogenase from *Thermoanaerobacter brockii* (TbADH) were purchased from Sigma. All reagents for site-directed mutagenesis experiments were purchased from New England Biolabs with the exception of oligonucleotides, which were purchased from Alta Bioscience (University of Birmingham, Birmingham, U.K.). H_2F was prepared by dithionite reduction of folate (*26*). NADPD was prepared by reduction of $NADP^+$ using d^8-2-propanol as the deuteride source and TbADH as the catalyst. The concentrations of NADPH/NADPD and H_2F were determined spectrophotometrically using extinction coefficients of 6200 cm^{-1} M^{-1} at 339 nm and 28000 cm^{-1} M^{-1} at 282 nm, respectively (*27*).

Site-Directed Mutagenesis. The four TmDHFR variants were created using the QuikChange site-directed mutagenesis kit (Stratagene) from a previously described pET11c-based expression vector containing the gene encoding TmDHFR (*12*). Mutagenic primers were 5′-CGGAAAGGGAATACCTTTTTTCGATAAGTTCGAAGGTTAC-3′ (E136K), 5′-CGATGAGTTCAAAGGTTACTTTCCTTTGAAACTTCTG-3′ (E138K), 5′-CGGAAAGGGAATACCTTTTTTCGATAAGTTCAAAGGTTACTTTCC-3′ (E136K/E138K), and 5′-CCGTACGTGTTCGGAGAGGGAATACCTTTTTTCG-3′ (K129E) (changes underlined). DNA sequences were confirmed by automated DNA sequencing (Functional Genomics Laboratory, School of Biosciences, University of Birmingham).

Protein Purification. BL21-CodonPlus(DE3)-RP cells (Stratagene) were used as the expression host for TmDHFR and its variants. Purification was conducted as described previously for wild-type TmDHFR (*12*) except that heat treatment was conducted at 70 °C. Heat treatment at 70 °C for 20 min did not significantly lower the DHFR activity of the crude solutions, indicating high thermostability in the TmDHFR variants. Purification on a HiPrep 16/10 SP XL cation-exchange column (GE Healthcare) led to essentially pure proteins as judged by sodium dodecyl sulfate−polyacrylamide gel electrophoresis (SDS−PAGE). Protein concentrations were determined spectroscopically assuming an average extinction coefficient for proteins of 20, 15, and 11 mL mg^{-1} cm^{-1} at 210, 215, and 220 nm, respectively (*28*).

Circular Dichroism Spectroscopy. Circular dichroism (CD) experiments were performed on an Applied Photophysics Chirascan circular dichroism spectrophotometer using protein concentrations of 10 μM in 5 mM potassium phosphate (pH 7.0) in a quartz cuvette (0.1 cm path length, Helma) under N_2. Mean residue ellipticities ($[\Theta]_{MRE}$) were calculated using the equation $[\Theta]_{MRE} = \Theta/(10ncl)$, where Θ is the measured ellipticity in millidegrees, n is the number of backbone amide bonds, c is the protein concentration in moles per liter, and l is the path length in centimeters. Thermal denaturation experiments were performed between 20 and 95 °C, with spectra recorded in temperature steps of 0.5 °C with a 1 min equilibration at the desired temperature prior to measurement. The melting temperature was determined by plotting $[\Theta]_{MRE}$ at 222 nm versus temperature. As had been seen for wild-type TmDHFR (*12*), thermal denaturation of the variants was irreversible.

Size Exclusion Chromatography. Size exclusion chromatography (SEC) was conducted to determine apparent molecular weights using a Superdex 75 10/300 GL column (GE Healthcare) at a flow rate of 0.5 mL/min. Enzyme concentrations of 10 or 100 μM in 100 mM potassium phosphate (pH 7.0) and 100 mM NaCl were used, in the absence and presence of 0.25% (w/v) CHAPS. Where appropriate, the enzyme was incubated with CHAPS for 60 min prior to injection onto the column. Varying the concentration of CHAPS (0.1−1%) did not affect the SEC profile. The column was calibrated and molecular weights determined as described previously (*13*).

Steady-State Kinetic Measurements. Turnover rates were measured spectrophotometrically by following the decrease in absorbance at 340 nm during the reaction [ε_{340}(NADPH + H_2F) = 11800 M^{-1} cm^{-1}] (*29*). Rates were determined at 20 and 40 °C in 100 mM potassium phosphate (pH 7.0) containing 100 mM NaCl. The enzyme (1 μM) was preincubated at the desired temperature with NADPH (100 μM) for 1 min to prevent hysteresis (*30*), prior to addition of H_2F (final concentration of 100 μM). Every data point is the result of three independent measurements. The calculated k_{cat} values are based on the number of binding sites (i.e., per monomer). Varying the concentrations of both substrate and cofactor (using 100 nM enzyme, which did not affect k_{cat}) between 0.5 and 100 μM showed that all K_m values were below 0.5 μM at 40 °C, as seen for the wild-type enzyme (*12*). Accurate K_m values could not be determined

because of the low reaction rates, which necessitated an overly high enzyme concentration to obtain good data while satisfying the Briggs−Haldane approximation. In addition, the pH dependence of k_{cat} was determined using saturating ligand concentrations at 40 °C in MTEN buffer (25 mM Tris, 25 mM ethanolamine, 50 mM MES, and 100 mm NaCl) between pH 4 and 9.

Pre-Steady-State Kinetic Measurements. Hydride transfer rates were measured under single-turnover conditions on an Applied Photophysics stopped-flow spectrophotometer essentially as described previously (*31*). The enzyme (final concentration of 20 μM) was preincubated with NADPH (final concentration of 8 μM) for at least 5 min in 100 mM potassium phosphate (pH 7.0) containing 100 mM NaCl, and the reaction was started by rapidly mixing this enzyme−cofactor complex with H_2F (final concentration of 200 μM) in the same buffer. Loss of fluorescence resonance energy transfer from the protein to NADPH during the reaction was observed by exciting the sample at 292 nm and measuring the emission using an output filter with a cutoff at 400 nm. All experiments were repeated nine times. Varying the concentrations of the reagents showed that the measured rates were limiting rates for hydride transfer.

RESULTS AND DISCUSSION

Design of the TmDHFR Salt Bridge Variants. To study the role of the three-way salt bridge among Lys129, Glu136, and Glu138 (Figure 1), we prepared three TmDHFR variants, TmDHFR-K129E, TmDHFR-E136K, and TmDHFR-E138K, in which these residues were singly replaced with an amino acid bearing an oppositely charged side chain. In addition, a TmDHFR-E136K/E138K variant was prepared to create the 'reverse' of the K129E mutation. The stabilizing salt bridge of wild-type TmDHFR would therefore be completely replaced with unfavorable anion−anion and cation−cation repulsive interactions in the TmDHFR-K129E and TmDHFR-E136K/E138K variants, respectively, while the E136K and E138K single variants would lead to partial disruption of the salt bridge. The use of four variants allows the role of the individual mutations to be separated from the overall effect on TmDHFR structure and catalysis. DNAs for the four TmDHFR salt bridge variants were generated by site-directed mutagenesis, expressed in *E. coli*, and the proteins purified as reported previously for the wild-type enzyme (*12*).

Quaternary Structure Determination by Size Exclusion Chromatography. The apparent molecular weights and hence the quaternary structure of the TmDHFR salt bridge variants under native conditions were measured by size exclusion chromatography (Figure 2 and the Supporting Information). All four variants eluted at approximately the same volume as wild-type TmDHFR, demonstrating that in all cases the dimer was the only detectable species in solution at concentrations of 100 μM. A 10-fold reduction of the protein concentration did not affect the elution volume. It has been shown previously that the nondenaturing zwitterionic detergent 3-[(3-cholamidopropyl)dimethylammonio]-1-propanesulfonate (CHAPS) can stabilize the monomer of TmDHFR-V11D so that this became the major species in solution (*13*). However, we found that addition of CHAPS to the salt bridge variants did not alter their elution profiles. The detergent cannot stabilize the monomers sufficiently to produce a significant solution population, unlike what was seen in the case of TmDHFR-V11D (*13*). The K129−E136−E138 salt bridge can therefore play only a minor role in dimerization of TmDHFR. Instead, it appears that hydrophobic interactions are the main driving force behind the formation of a strong TmDHFR dimer (*13*).

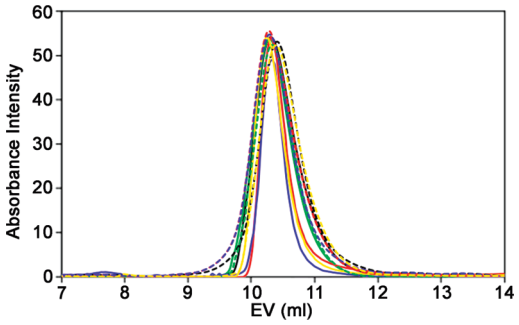

FIGURE 2: Size exclusion chromatography of 100 μM TmDHFR (black), TmDHFR-K129E (green), TmDHFR-E136K (red), TmDHFR-E138K (blue), and TmDHFR-E136K/E138K (orange) in 100 mM potassium phosphate containing 100 mM NaCl in the absence (solid lines) and presence (dotted lines) of 0.25% CHAPS.

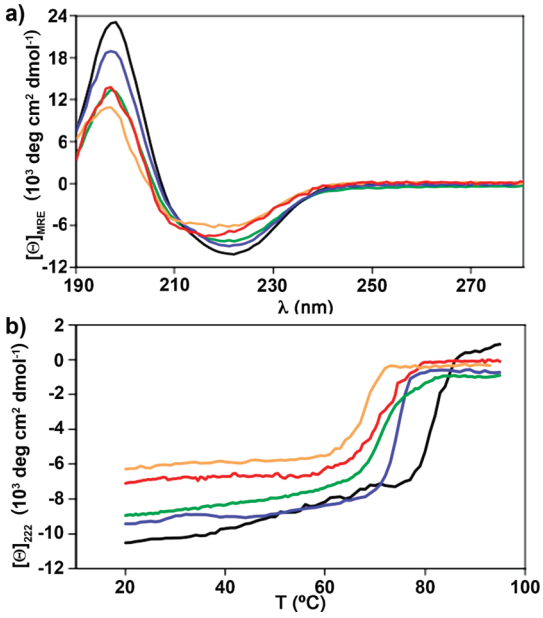

FIGURE 3: CD spectra at 20 °C (a) and thermal denaturation profiles (b) of 10 μM TmDHFR (black), TmDHFR-K129E (green), TmDHFR-E136K (red), TmDHFR-E138K (blue), and TmDHFR-E136K/E138K (orange) in 5 mM potassium phosphate (pH 7).

Conformational Analysis by CD Spectroscopy. Far-UV CD spectra were recorded for all four TmDHFR variants (Figure 3A and Table 1). The CD spectra of TmDHFR-K129E and TmDHFR-E138K were similar in appearance to that of the wild-type enzyme, with minimum mean residue ellipticities ($[\Theta]_{MRE}$) at 222 nm of −8290 ± 150 and −8820 ± 190 deg cm^2 dmol^{-1}, respectively, compared to −10140 ± 130 deg cm^2 dmol^{-1} for wild-type TmDHFR. The CD spectra of TmDHFR-E136K and TmDHFR-E136K/E138K on the other hand were blue-shifted relative to that of wild-type TmDHFR, giving $[\Theta]_{MRE}$ at 218 nm of −7507 ± 142 and −6285 ± 193 deg cm^2 dmol^{-1} residue^{-1}, respectively. This shows that while the secondary structure of TmDHFR is robust to the K129E and E138K substitutions and hence to disruption of the salt bridge, the E136K substitution has a significant effect.

CD spectroscopy was also used to investigate the thermal stability of the four TmDHFR variants (Figure 3B and Table 1).

Table 1: Comparison of Wild-Type (WT) TmDHFR and Its Salt Bridge Variants[a]

	WT	K129E	E136K	E138K	E136K/E138K
MRE[b] (deg cm^2 dmol^{-1})	−10140 ± 130	−8290 ± 150	−6930 ± 170	−8820 ± 190	−5960 ± 210
T_m (°C)	81.5 ± 0.4	71.5 ± 1.1	71.3 ± 0.7	75.0 ± 0.8	68.1 ± 0.8
k_{cat}[b] (s^{-1})	0.123 ± 0.011	0.115 ± 0.007	0.058 ± 0.005	0.104 ± 0.009	0.018 ± 0.002
pK_a[c]	5.98 ± 0.07	6.31 ± 0.04	6.38 ± 0.11	6.28 ± 0.09	6.53 ± 0.06
k_H[b] (s^{-1})	0.122 ± 0.003	0.124 ± 0.002	0.104 ± 0.003	0.143 ± 0.003	0.087 ± 0.010
KIE_{k_H}[d]	3.95 ± 0.24	3.12 ± 0.24	3.13 ± 0.12	3.06 ± 0.30	3.18 ± 0.32
E_a (kJ mol^{-1})	53.5 ± 0.4[e]	53.2 ± 0.5	53.5 ± 0.3	53.3 ± 0.3	53.8 ± 0.4
ΔE_a (kJ mol^{-1})	2.5 ± 1.0[e]	2.8 ± 0.7	0.3 ± 0.4	1.1 ± 0.4	−0.1 ± 0.6
A_H (s^{-1})	(4.1 ± 0.7) × 10^{8}[e]	(1.2 ± 0.2) × 10^{8}	(1.3 ± 0.1) × 10^{8}	(2.3 ± 0.2) × 10^{8}	(1.1 ± 0.2) × 10^{8}
A_H/A_D	1.6 ± 0.5[e]	1.1 ± 0.3	2.8 ± 0.4	2.0 ± 0.3	1.2 ± 0.2

[a]MRE is the mean residue ellipticity at 222 nm. T_m is the thermal melting temperature. k_{cat} is the steady-state rate constant. pK_a is the apparent pK_a on k_{cat}. k_H is the hydride transfer rate constant (pre-steady-state conditions). KIE_{k_H} is the primary kinetic isotope effect on hydride transfer. E_a is the activation energy for hydride transfer. ΔE_a is the activation energy difference between hydride and deuteride transfer. A_H is the Arrhenius prefactor for k_H. A_H/A_D is the ratio of Arrhenius prefactors for hydride and deuteride transfer. [b]At 20 °C. [c]At 40 °C. [d]Average over the temperature-independent region. [e]At > 25 °C.

As had been observed for the wild-type enzyme, all variants showed a single denaturation transition (Figure 3B) consistent with a two-state folded dimer to unfolded monomer transition with no folded monomer (*11*). This provides further evidence that disruption of the salt bridge does not significantly impair dimerization of TmDHFR even at elevated temperatures. The E138K single mutation had a significant effect on the thermostability of the enzyme causing a reduction of more than 6 °C in the melting temperature. As one would expect because of the complete loss of the salt bridge, the K129E mutation had a greater effect, leading to a 10 °C reduction in the thermal stability. As was seen for the CD spectra, the E136K mutation had a larger effect on the thermal stability of TmDHFR than the E138K mutation, while TmDHFR-E136K/E138K showed the lowest melting temperature of the four variants (Table 1). This provides further evidence that the structure of TmDHFR-E136K is compromised beyond simply the loss of a salt bridge interaction, suggesting a longer-range structural change. The loss of thermostability seen in the salt bridge variants was considerably less pronounced than that observed for the two hydrophobic interface variants TmDHFR-V11D and TmDHFR-V126E (*13*), although a 10 °C reduction in the thermal melting point is still a significant change and one that would most likely lead to a loss of viability of TmDHFR at the elevated temperatures at which *T. maritima* lives.

Kinetic Measurements. Steady-state turnover rates at 20 °C and pH 7 (Table 1) were found to be approximately the same for wild-type TmDHFR, TmDHFR-K129E, and TmDHFR-E138K, demonstrating that the disruption of the salt bridge did not affect catalysis. k_{cat} values were reduced for TmDHFR-E136K and TmDHFR-E136K/E138K between 2- and 10-fold, in further agreement with the structural perturbations described above where the E136K mutation had a larger effect than the K129E and E138K mutations. All K_m values were less than 0.5 μM (Supporting Information), as had been seen previously for the wild-type enzyme (*13*, *14*).

Hydride transfer rate constants k_H, measured under single-turnover transient-state conditions that isolate the chemical step of the catalytic cycle, showed little difference between TmDHFR and its salt bridge variants (Figure 4, Table 1, and the Supporting Information). The temperature dependence of k_H revealed little difference across the temperature range of 5−65 °C and approximately equal activation energies for TmDHFR and the four variants. This suggests that the larger differences seen for k_{cat} are the result of effects on physical steps in the catalytic cycle.

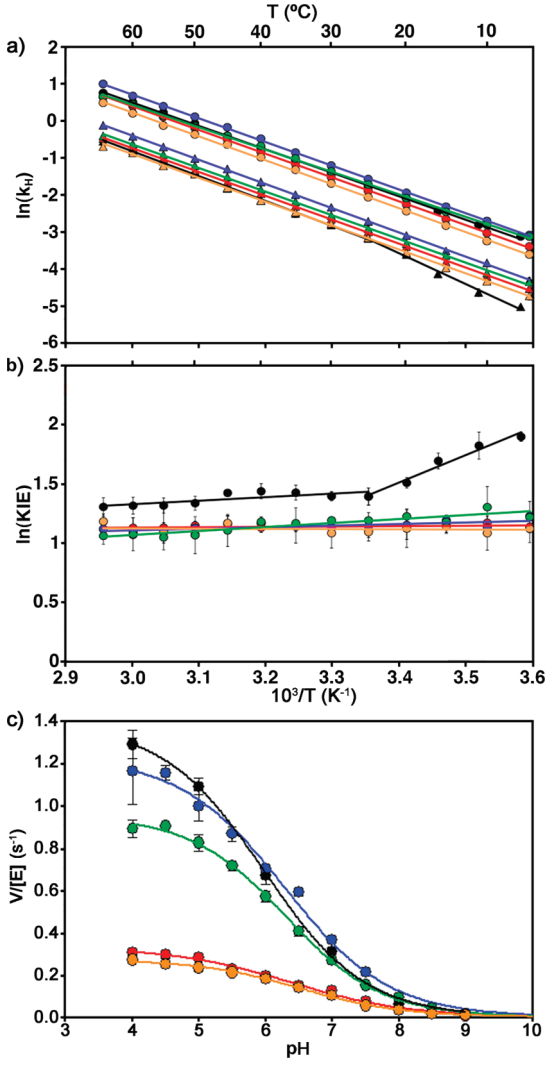

FIGURE 4: Arrhenius plots for k_H (circles) and k_D (triangles) (a), logarithmic plot of the KIE on k_H (b), and pH dependence of the steady-state turnover rate at 40 °C (c) for catalysis by TmDHFR (black), TmDHFR-K129E (green), TmDHFR-E136K (red), TmDHFR-E138K (blue), and TmDHFR-E136K/E138K (orange).

The pH dependence of k_{cat} was determined at 40 °C (Figure 4 and the Supporting Information). All four variants exhibited a slight increase in the apparent pK_a compared to that of the wild-type enzyme (Table 1), which is also likely to be due to the effect of the mutations on physical steps in the

catalytic cycle. If k_{cat} is directly affected by the swapping of acidic glutamate and basic lysine side chains, then this effect cannot be predicted on the basis of the number of each type of residue.

A much more significant effect was seen for the rates of deuteride transfer, k_D, and hence the primary kinetic isotope effects (KIEs) (Figure 4 and the Supporting Information). k_D was elevated slightly in all four salt bridge variants compared to that of wild-type TmDHFR and did not show the striking breakpoint in its temperature dependence that had been seen for the wild-type enzyme (*31*). The salt bridge variants therefore displayed a monophasic temperature dependence of their primary KIEs with slightly depressed KIEs compared to wild-type TmDHFR. The magnitude and temperature dependence of the KIEs for the salt bridge variants closely resembled those observed for wild-type TmDHFR in the presence of high concentrations of sucrose (*32*). This lends further support to the hypothesis that the breakpoint in the temperature dependence of the KIE is intimately related to the dimer interface of TmDHFR, and that high concentrations of sucrose exert specific effects at the dimer interface (*32*). Sucrose did not have a significant effect on the KIE in the monomeric DHFR from *E. coli* (*33*).

The temperature dependence of the KIE is often interpreted in terms of the coupling of protein motions to the reaction coordinate, with temperature-dependent KIEs being indicative of short-range "promoting motions" that narrow the reaction barrier (in addition to reducing its height); such barrier compressing motions have been described in frameworks called rate-promoting vibrations (*34*), environmentally coupled tunneling (*35*, *36*), vibrationally enhanced ground-state tunneling (*37*), and multidimensional tunneling (*38*). Others have presented evidence of a role for short-range promoting motions in other enzymes (*39*−*41*). However, the fully temperature independent KIEs seen for the TmDHFR salt bridge variants would suggest that these short-range motions are lost (or their role negated) in the mutants described here, implying a long-range effect on a short-range motion. In contrast, the similarity between the temperature dependence of the KIE in the presence of sucrose (*32*) and in the salt bridge mutants demonstrates that catalysis in TmDHFR is unaffected by viscosity and, hence, that long-range coupled motions do not play a role in the chemical step of the TmDHFR- and EcDHFR-catalyzed reactions as previously suggested (*3*, *42*). Instead, it is possible that disruption of the salt bridge (or binding of polyols to this region) affects the conformational ensemble of TmDHFR. It has previously been shown that mutations to the homologous loop region of EcDHFR affect the conformational ensemble and that this may be the cause of the diminished catalytic performance of these mutants (*43*). Computational studies have also shown that the catalytic behavior of EcDHFR can be explained by changes to the populations of conformational substates rather than by "promoting motions" (*44*−*47*). Long-range correlations in EcDHFR could be quasi-thermodynamic, and altering the conformational ensemble could be considered a long-range, viscosity-independent effect. Interestingly, of the two hydrophobic interface mutants previously reported, TmDHFR-V11D exhibited a monophasic temperature dependence of the KIE on hydride transfer while the behavior of the KIE of TmDHFR-V126E resembled that of the wild-type enzyme (*13*).

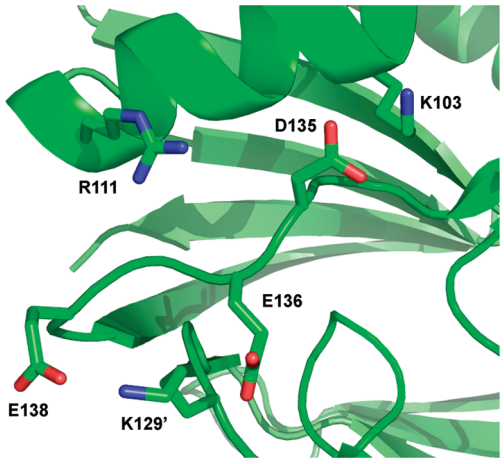

FIGURE 5: Cartoon representation of TmDHFR showing surface ionic residues (shown as sticks) in the vicinity of the K129−E136−E138 salt bridge, created from Protein Data Bank entry 1D1G (*9*) using PyMOL.

CONCLUSIONS

The results presented here demonstrate that the three-membered salt bridge (K129−E136−E138) in TmDHFR is not important for dimer formation, although it does contribute significantly to the high thermal stability of the enzyme. Intersubunit ion pairs have been shown to improve enzyme thermostability (*21*−*24*), although their role in promoting oligomerization has also been demonstrated (*21*). The recently determined crystal structure of an exopolygalacturonase from *T. maritima* shows that this enzyme, unlike other polygalacturonases, is a tetramer in solution and that the tetramer interface involves an intermolecular parallel β-strand with four flanking ion pairs to form a dimer, with an extensive hydrophobic interface between the two dimers (*48*). Given the scale of the hydrogen bonding and hydrophobic portions of the interface, it seems likely that the ion pairs play a minor role in oligomerization in this case also.

In DHFR from *Thermotoga petrophila* (TpDHFR), which is 94% identical and 98% similar to TmDHFR, the K129−E136−E138 salt bridge is conserved (*49*), whereas in DHFR from *Thermotoga neapolitana* (TnDHFR, 75% identical and 90% similar to TmDHFR), residue 129 is arginine and residue 136 is aspartate (*50*). A three-membered salt bridge is therefore present in all three DHFRs, although it is modified in TnDHFR. All three species have similar growth temperature maxima and optima (*51*−*53*), so there is no obvious advantage to this modification in terms of thermal stability. The residues of the dimer interface are extensively conserved among the three enzymes, with most substitutions occurring in surface loop regions away from the interface (Supporting Information).

The disproportionate effect of the E136K mutation on TmDHFR compared to the E138K mutation may be due to the presence of D135, which forms an intrasubunit salt bridge with K103 in the wild-type enzyme. In the E136K variant, K136 may move toward this salt bridge to avoid K129′ and R111 (Figure 5), disrupting the original interaction and causing a conformational change in the enzyme. As there are no other charged residues in the vicinity of K129 and E138, their replacement with oppositely charged side chains would not be expected to have such a large effect.

It appears therefore that the dimer interface of TmDHFR is entirely dominated by the hydrophobic interaction between the buried portions of the interface and that the peripheral

intersubunit salt bridges do not play an important role in dimer formation. This is similar to dimeric phosphoribosylanthranilate isomerase from *T. maritima*, which can also be converted to a functional monomer by disruption of the hydrophobic interface despite the presence of intersubunit salt bridges (*16*). However, in the case of TmDHFR, these intersubunit salt bridges are vital for maintaining the high thermal stability required for the enzyme to function at biologically extreme temperatures.

The rate of dihydrofolate reduction by TmDHFR is not significantly affected by the loss of the K129−E136−E138 salt bridge. Changes to the temperature dependence of the KIE on hydride transfer are in agreement with our recent results (*33*) which suggest that DHFR catalysis is affected by changes to the conformational ensemble of the enzyme rather than only the coupling of protein motions to the reaction coordinate.

ACKNOWLEDGMENT

We thank Robert J. Rodriguez for help with the initial phase of this project.

SUPPORTING INFORMATION AVAILABLE

Amino acid sequence alignment of TmDHFR, TnDHFR, and TpDHFR; Michaelis−Menten plots; and tabulated data from size exclusion chromatography, k_{cat} versus pH, and k_H, k_D, and KIE_{k_H} versus temperature. This material is available free of charge via the Internet at http://pubs.acs.org.

REFERENCES

1. Allemann, R. K., Evans, R. M., and Loveridge, E. J. (2009) Probing coupled motions in enzymatic hydrogen tunnelling reactions. *Biochem. Soc. Trans. 37*, 349–353.
2. Allemann, R. K., Evans, R. M., Tey, L. H., Maglia, G., Pang, J. Y., Rodriguez, R., Shrimpton, P. J., and Swanwick, R. S. (2006) Protein motions during catalysis by dihydrofolate reductases. *Philos. Trans. R. Soc. London, Ser. B 361*, 1317–1321.
3. Benkovic, S. J., and Hammes-Schiffer, S. (2006) Biochemistry: Enzyme motions inside and out. *Science 312*, 208–209.
4. Boehr, D. D., McElheny, D., Dyson, H. J., and Wright, P. E. (2006) The dynamic energy landscape of dihydrofolate reductase catalysis. *Science 313*, 1638–1642.
5. Mauldin, R. V., Carroll, M. J., and Lee, A. L. (2009) Dynamic Dysfunction in Dihydrofolate Reductase Results from Antifolate Drug Binding: Modulation of Dynamics within a Structural State. *Structure 17*, 386–394.
6. Iwakura, M., Maki, K., Takahashi, H., Takenawa, T., Yokota, A., Katayanagi, K., Kamiyama, T., and Gekko, K. (2006) Evolutional design of a hyperactive cysteine- and methionine-free mutant of *Escherichia coli* dihydrofolate reductase. *J. Biol. Chem. 281*, 13234–13246.
7. Liu, H. B., and Warshel, A. (2007) The catalytic effect of dihydrofolate reductase and its mutants is determined by reorganization energies. *Biochemistry 46*, 6011–6025.
8. Wilquet, V., Gaspar, J. A., van de Lande, M., van de Casteele, M., Legrain, C., Meiering, E. M., and Glansdorff, N. (1998) Purification and characterization of recombinant *Thermotoga maritima* dihydrofolate reductase. *Eur. J. Biochem. 255*, 628–637.
9. Dams, T., Auerbach, G., Bader, G., Jacob, U., Ploom, T., Huber, R., and Jaenicke, R. (2000) The crystal structure of dihydrofolate reductase from *Thermotoga maritima*: Molecular features of thermostability. *J. Mol. Biol. 297*, 659–672.
10. Dams, T., Bohm, G., Auerbach, G., Bader, G., Schurig, H., and Jaenicke, R. (1998) Homo-dimeric recombinant dihydrofolate reductase from *Thermotoga maritima* shows extreme intrinsic stability. *Biol. Chem. 379*, 367–371.
11. Dams, T., and Jaenicke, R. (1999) Stability and folding of dihydrofolate reductase from the hyperthermophilic bacterium *Thermotoga maritima*. *Biochemistry 38*, 9169–9178.
12. Maglia, G., Javed, M. H., and Allemann, R. K. (2003) Hydride transfer during catalysis by dihydrofolate reductase from *Thermotoga maritima*. *Biochem. J. 374*, 529–535.
13. Loveridge, E. J., Rodriguez, R. J., Swanwick, R. S., and Allemann, R. K. (2009) Effect of Dimerisation on the Stability and Catalytic Activity of Dihydrofolate Reductase from the Hyperthermophile *Thermotoga maritima*. *Biochemistry 48*, 5922–5933.
14. Loveridge, E. J., Maglia, G., and Allemann, R. K. (2009) The Role of Arginine 28 in Catalysis by Dihydrofolate Reductase from the Hyperthermophile *Thermotoga maritima*. *ChemBioChem 10*, 2624–2627.
15. Pang, J. Y., Pu, J. Z., Gao, J. L., Truhlar, D. G., and Allemann, R. K. (2006) Hydride transfer reaction catalyzed by hyperthermophilic dihydrofolate reductase is dominated by quantum mechanical tunneling and is promoted by both inter- and intramonomeric correlated motions. *J. Am. Chem. Soc. 128*, 8015–8023.
16. Thoma, R., Hennig, M., Sterner, R., and Kirschner, K. (2000) Structure and function of mutationally generated monomers of dimeric phosphoribosylanthranilate isomerase from *Thermotoga maritima*. *Struct. Folding Des. 8*, 265–276.
17. Vieille, C., and Zeikus, G. J. (2001) Hyperthermophilic Enzymes: Sources, Uses, and Molecular Mechanisms for Thermostability. *Microbiol. Mol. Biol. Rev. 65*, 1–43.
18. Robinson-Rechavi, M., Alibes, A., and Godzik, A. (2006) Contribution of electrostatic interactions, compactness and quaternary structure to protein thermostability: Lessons from structural genomics of *Thermotoga maritima*. *J. Mol. Biol. 356*, 547–557.
19. Merz, A., Knöchel, T., Jansonius, J. N., and Kirschner, K. (1999) The hyperthermostable indoleglycerol phosphate synthase from *Thermotoga maritima* is destabilized by mutational disruption of two solvent-exposed salt bridges. *J. Mol. Biol. 288*, 753–763.
20. Pappenberger, G., Schurig, H., and Jaenicke, R. (1997) Disruption of an ionic network leads to accelerated thermal denaturation of D-glyceraldehyde-3-phosphate dehydrogenase from the hyperthermophilic bacterium *Thermotoga maritima*. *J. Mol. Biol. 274*, 676–683.
21. Binter, A., Staunig, N., Jelesarov, I., Lohner, K., Palfey, B. A., Deller, S., Gruber, K., and Macheroux, P. (2009) A single intersubunit salt bridge affects oligomerization and catalytic activity in a bacterial quinone reductase. *FEBS J. 276*, 5263–5274.
22. Rahman, R. N. Z. A., Fujiwara, S., Nakamura, H., Takagi, M., and Imanaka, T. (1998) Ion Pairs Involved in Maintaining a Thermostable Structure of Glutamate Dehydrogenase from a Hyperthermophilic Archaeon. *Biochem. Biophys. Res. Commun. 248*, 920–926.
23. Vetriani, C., Maeder, D. L., Tolliday, N., Yip, K. S.-P., Stillman, T. J., Britton, K. L., Rice, D. W., Klump, H. H., and Robb, F. T. (1998) Protein thermostability above 100 °C: A key role for ionic interactions. *Proc. Natl. Acad. Sci. U.S.A. 95*, 12300–12305.
24. Goihberg, E., Peretz, M., Tel-Or, S., Dym, O., Shimon, L., Frolow, F., and Burstein, Y. (2010) Biochemical and Structural Properties of Chimeras Constructed by Exchange of Cofactor-Binding Domains in Alcohol Dehydrogenases from Thermophilic and Mesophilic Microorganisms. *Biochemistry 49*, 1943–1953.
25. Pang, J. Y., and Allemann, R. K. (2007) Molecular dynamics simulation of thermal unfolding of *Thermatoga maritima* DHFR. *Phys. Chem. Chem. Phys. 9*, 711–718.
26. Blakley, R. L. (1960) Crystalline dihydropteroylglutamic acid. *Nature 188*, 231–232.
27. Swanwick, R. S., Maglia, G., Tey, L., and Allemann, R. K. (2006) Coupling of protein motions and hydrogen transfer during catalysis by *Escherichia coli* dihydrofolate reductase. *Biochem. J. 394*, 259–265.
28. Scopes, R. R. (1994) Protein Purification: Principles and Practice, 3rd ed., Springer-Verlag, Inc., New York.
29. Stone, S. R., and Morrison, J. F. (1982) Kinetic mechanism of the reaction catalyzed by dihydrofolate reductase from *Escherichia coli*. *Biochemistry 21*, 3757–3765.
30. Fierke, C. A., Johnson, K. A., and Benkovic, S. J. (1987) Construction and Evaluation of the Kinetic Scheme Associated with Dihydrofolate Reductase from *Escherichia coli*. *Biochemistry 26*, 4085–4092.
31. Maglia, G., and Allemann, R. K. (2003) Evidence for environmentally coupled hydrogen tunneling during dihydrofolate reductase catalysis. *J. Am. Chem. Soc. 125*, 13372–13373.
32. Loveridge, E. J., Evans, R. M., and Allemann, R. K. (2008) Solvent Effects on Environmentally Coupled Hydrogen Tunnelling During Catalysis by Dihydrofolate Reductase from *Thermotoga maritima*. *Chem.—Eur. J. 14*, 10782–10788.
33. Loveridge, E. J., Tey, L. H., and Allemann, R. K. (2010) Solvent Effects on Catalysis by *Escherichia coli* Dihydrofolate Reductase. *J. Am. Chem. Soc. 132*, 1137–1143.
34. Antoniou, D., Caratzoulas, S., Kalyanaraman, C., Mincer, J. S., and Schwartz, S. D. (2002) Barrier passage and protein dynamics in enzymatically catalyzed reactions. *Eur. J. Biochem. 269*, 3103–3112.

35. Knapp, M. J., and Klinman, J. P. (2002) Environmentally coupled hydrogen tunneling: Linking catalysis to dynamics. *Eur. J. Biochem. 269*, 3113–3121.
36. Nagel, Z. D., and Klinman, J. P. (2006) Tunneling and dynamics in enzymatic hydride transfer. *Chem. Rev. 106*, 3095–3118.
37. Sutcliffe, M. J., and Scrutton, N. S. (2002) A new conceptual framework for enzyme catalysis: Hydrogen tunneling coupled to enzyme dynamics in flavoprotein and quinoprotein enzymes. *Eur. J. Biochem. 269*, 3096–3102.
38. Truhlar, D. (2006) Variational transition state theory and multidimensional tunneling for simple and complex reactions in the gas phase, solids, liquids and enzymes, in *Isotope Effect in Chemistry and Biology* (Kohen A. and Limbach H.-H., Eds.) CRC/Taylor and Francis, Boca Raton, FL.
39. Nunez, S., Antoniou, D., Schramm, V. L., and Schwartz, S. D. (2004) Promoting Vibrations in Human Purine Nucleoside Phosphorylase. A Molecular Dynamics and Hybrid Quantum Mechanical/Molecular Mechanical Study. *J. Am. Chem. Soc. 126*, 15720–15729.
40. Masgrau, L., Roujeinikova, A., Johannissen, L. O., Hothi, P., Basran, J., Ranaghan, K. E., Mulholland, A. J., Sutcliffe, M. J., Scrutton, N. S., and Leys, D. (2006) Atomic description of an enzyme reaction dominated by proton tunneling. *Science 312*, 237–241.
41. Pudney, C. R., Hay, S., Levy, C., Pang, J., Sutcliffe, M. J., Leys, D., and Scrutton, N. S. (2009) Evidence To Support the Hypothesis That Promoting Vibrations Enhance the Rate of an Enzyme Catalyzed H-Tunneling Reaction. *J. Am. Chem. Soc. 131*, 17072–17073.
42. Agarwal, P. K., Billeter, S. R., Rajagopalan, P. T. R., Benkovic, S. J., and Hammes-Schiffer, S. (2002) Network of coupled promoting motions in enzyme catalysis. *Proc. Natl. Acad. Sci. U.S.A. 99*, 2794–2799.
43. Swanwick, R. S., Shrimpton, P. J., and Allemann, R. K. (2004) Pivotal role of Gly 121 in dihydrofolate reductase from *Escherichia coli*: The altered structure of a mutant enzyme may form the basis of its diminished catalytic performance. *Biochemistry 43*, 4119–4127.
44. Agarwal, P. K., Billeter, S. R., and Hammes-Schiffer, S. (2002) Nuclear quantum effects and enzyme dynamics in dihydrofolate reductase catalysis. *J. Phys. Chem. B 106*, 3283–3293.
45. Garcia-Viloca, M., Truhlar, D. G., and Gao, J. (2003) Reaction-path energetics and kinetics of the hydride transfer reaction catalyzed by dihydrofolate reductase. *Biochemistry 42*, 13558–13575.
46. Thorpe, I. F., and Brooks, C. L. (2004) The coupling of structural fluctuations to hydride transfer in dihydrofolate reductase. *Proteins 57*, 444–457.
47. Thorpe, I. F., and Brooks, C. L. (2005) Conformational substates modulate hydride transfer in dihydrofolate reductase. *J. Am. Chem. Soc. 127*, 12997–13006.
48. Pijning, T., van Pouderoyen, G., Kluskens, L., van der Oost, J., and Dijkstra, B. W. (2009) The crystal structure of a hyperthermoactive exopolygalacturonase from *Thermotoga maritima* reveals a unique tetramer. *FEBS Lett. 583*, 3665–3670.
49. http://cmr.jcvi.org/cgi-bin/CMR/GenomePage.cgi?org = nttp02.
50. DeBoy, R. T., Mongodin, E. F., Emerson, J. B., and Nelson, K. E. (2006) Chromosome evolution in the Thermotogales: Large-scale inversions and strain diversification of CRISPR sequences. *J. Bacteriol. 188*, 2364–2374.
51. Huber, R., Langworthy, T. A., König, H., Thomm, M., Woese, C. R., Sleytr, U. B., and Stetter, K. O. (1986) *Thermotoga maritima* sp. nov. represents a new genus of unique extremely thermophilic eubacteria growing up to 90 °C. *Arch. Microbiol. 144*, 324–333.
52. Jannasch, H. W., Huber, R., Belkin, S., and Stetter, K. O. (1988) *Thermotoga neapolitana* sp. nov. of the extremely thermophilic, eubacterial genus *Thermotoga*. *Arch. Microbiol. 150*, 103–104.
53. Takahata, Y., Nishijima, M., Hoaki, T., and Maruyama, T. (2001) *Thermotoga petrophila* sp. nov. and *Thermotoga naphthophila* sp. nov., two hyperthermophilic bacteria from the Kubiki oil reservoir in Niigata, Japan. *Int. J. Syst. Evol. Microbiol. 51*, 1901–1909.